IOP Publishing — Science and Technology of Advanced Materials
Sci. Technol. Adv. Mater. **11** (2010) 065002 (6pp) doi:10.1088/1468-6996/11/6/065002

Voltage- and current-activated metal–insulator transition in VO_2-based electrical switches: a lifetime operation analysis

Aurelian Crunteanu[1], Julien Givernaud[1], Jonathan Leroy[1], David Mardivirin[1], Corinne Champeaux[2], Jean-Christophe Orlianges[2], Alain Catherinot[1] and Pierre Blondy[1]

[1] XLIM Research Institute UMR no. 6172, CNRS/ Université de Limoges, 123 avenue Albert Thomas, 87060 Limoges, France
[2] SPCTS UMR no. 6638, CNRS/ Université de Limoges, 123 avenue Albert Thomas, 87060 Limoges, France

E-mail: aurelian.crunteanu@xlim.fr

Received 20 August 2010
Accepted for publication 24 October 2010
Published 2 December 2010
Online at stacks.iop.org/STAM/11/065002

Abstract
Vanadium dioxide is an intensively studied material that undergoes a temperature-induced metal–insulator phase transition accompanied by a large change in electrical resistivity. Electrical switches based on this material show promising properties in terms of speed and broadband operation. The exploration of the failure behavior and reliability of such devices is very important in view of their integration in practical electronic circuits. We performed systematic lifetime investigations of two-terminal switches based on the electrical activation of the metal–insulator transition in VO_2 thin films. The devices were integrated in coplanar microwave waveguides (CPWs) in series configuration. We detected the evolution of a 10 GHz microwave signal transmitted through the CPW, modulated by the activation of the VO_2 switches in both voltage- and current-controlled modes. We demonstrated enhanced lifetime operation of current-controlled VO_2-based switching (more than 260 million cycles without failure) compared with the voltage-activated mode (breakdown at around 16 million activation cycles). The evolution of the electrical self-oscillations of a VO_2-based switch induced in the current-operated mode is a subtle indicator of the material properties modification and can be used to monitor its behavior under various external stresses in sensor applications.

Keywords: vanadium dioxide, electrical switching, metal–insulator transition, lifetime operation

1. Introduction

Vanadium dioxide (VO_2) exhibits a reversible temperature-driven metal–insulator transition (MIT), which markedly changes its electronic and optical properties [1, 2]. Below the transition temperature of ∼68 °C, VO_2 behaves as an insulator or semiconductor with a monoclinic crystal structure and a band gap of about 1 eV, whereas for temperatures higher than 68 °C, it transforms abruptly to a metallic state with a tetragonal rutile structure. In VO_2 thin films, this transition can be triggered by thermal [1–3], electrical (charge injection or Joule heating) [2–4] or optical excitation (photon excitation) [5, 6], and even by external pressure or strain [7]. The MIT induces extremely fast and abrupt changes in the electronic and optical properties of the material: the electrical resistivity increases by 3 to 5 orders of magnitude (depending on the crystalline quality of the deposited films [8], stoichiometry and doping [9]) while the optical reflectivity markedly decreases [5, 6]. An activation time as short as 100 fs has been reported for the optically driven MIT transition [5, 6], and the electronically induced transition occurs within nanoseconds [2–4, 10]. The physical mechanisms underlying the MIT in VO_2 are not fully elucidated and it is still unclear whether the transition is driven by the crystalline phase transition (from monoclinic to the tetragonal phase) or by electron–electron correlations (pure electronic Mott transition), although recent reports apparently favor the second mechanism [11]. The remarkable properties and broadband operation of the MIT in VO_2 have received ever-increasing attention from the scientific community during the last few years and have made the material an interesting candidate for fast switching with feasible applications in domains spanning over the entire electromagnetic spectrum. These applications include low-frequency two- and three-terminal electrical switches [2–4], RF-microwave switches, tunable filters [10, 12] and power limiters [13], THz metamaterial devices [14, 15] and nanoresonators [16] and optical [5, 6] components.

For the realization of practical devices, the electrical activation of VO_2 (in two- or three-terminal configurations) is favored over the thermal one as it offers faster activation times and easier implementation. However, the literature on the lifetime and reliability of such components is scarce. An early study by Guzman *et al* [17] on the electrical characteristics of VO_2 thin films obtained by the sol–gel method showed that their MIT switching properties were unaffected after 108 Joule-heating activation cycles. On the other hand, Ilinski *et al* [18] observed a rapid degradation and suppression of the MIT hysteresis loops in the electrical conductivity and optical reflectivity of amorphous VO_2 thin films after only a few thermal cycles across the phase transition region. More recently, Ko and Ramanathan [19] have shown that the MIT characteristics of high-quality polycrystalline VO_2 thin films were largely unaffected after 102 thermal cycles over the phase transition. It was suggested [19] that during thermocycling, the polycrystalline structure of VO_2 thin films prevents microcrack formation and hinders oxygen diffusion from VO_2 clusters to the nearby low-oxygen regions, as observed in the amorphous films.

Studies on the effect of recurrent electrical activation of VO_2 switches on their properties have not yet been reported. Therefore, in this paper, we present a methodical investigation on the reliability and lifetime of electrical switching based on the MIT in VO_2 thin films.

2. Experimental details

We fabricated two-terminal devices using VO_2 thin films obtained by pulsed laser deposition (PLD), which were further integrated in coplanar microwave waveguides (CPWs) [10]. We recorded the evolution of a continuous microwave (MW) signal at 10 GHz traveling through a microwave guide during the sequential activation of a VO_2 device. Using this detection method, we aimed to avoid interference and feedback between the detected signal and the actuation of the VO_2-based switches.

VO_2 thin films were deposited using reactive PLD from a high-purity (99.95%) vanadium target under an oxygen atmosphere on Al_2O_3 *c*-type substrates. The experimental conditions are detailed elsewhere [10, 12]. The obtained 200-nm-thick VO_2 films were crystalline and showed a change in resistivity of about 5 orders of magnitude during a thermally induced MIT [12]. The two-terminal VO_2 switches were fabricated in a clean room environment [10, 12]: VO_2 rectangular patterns with different dimensions were defined lithographically, and gold electrodes were deposited and patterned on the VO_2 patterns. The electrode width was 20 μm and the spacing was varied between 5 and 50 μm. Current–voltage (I–V) characteristics of the two-terminal devices were recorded using a Keithley 2612A source meter in voltage or current mode.

3. Results and discussion

3.1. Characterization of VO_2-based two-terminal devices

Figure 1(a) shows the I–V curves (V-mode and I-mode) of a typical VO_2 switch of 20 μm length and 20 μm width. The switch was integrated in the simple measurement setup depicted in the inset of figure 1(a), in series with a 1 kΩ resistance (R_s) and the voltage or current source. Both I–V characteristics are highly nonlinear. In the V-mode operation, when the voltage is raised to the threshold value V_s, the VO_2 transforms abruptly from the highly resistive insulator state (point S on the I–V curve) to the low-resistive metallic state (point M). Consequently, the current jumps from ∼2.2 to 46 mA. By further increasing the applied voltage beyond point M, the V-mode I–V trace follows an ohmic linear law. When decreasing the voltage, the V-mode trace shows a large hysteresis loop ($\Delta V = 17.5$ V) until reaching point M* where VO_2 transforms back to a semiconductor. The width of the hysteresis indicates an MIT transition mediated by Joule heating [3, 4, 12]. The I-mode trace is expanded in figure 1(b) with the red arrow (blue) curves corresponding to the increasing (decreasing) current between 0 and 10 mA. The clear S-type shape reveals a region of negative differential resistance (NDR) between the instability points S and M*. It was suggested that the onset of the NDR corresponds to the MIT in a percolative manner, with the coexistence of the semiconducting and metallic domains in VO_2 [3, 4, 20]. Figure 1(b) reveals that the I-mode I–V curve has a narrower hysteresis (which even disappears for devices with lengths shorter than 10 μm), indicating that, in this case, the MIT is mainly triggered by charge injection with less heat generation.

3.2. Coplanar microwave waveguides integrating VO_2 switches

We integrated the VO_2 electrical switches with the I–V characteristics shown in figure 1 to coplanar microwave waveguides in a series configuration, with a central signal

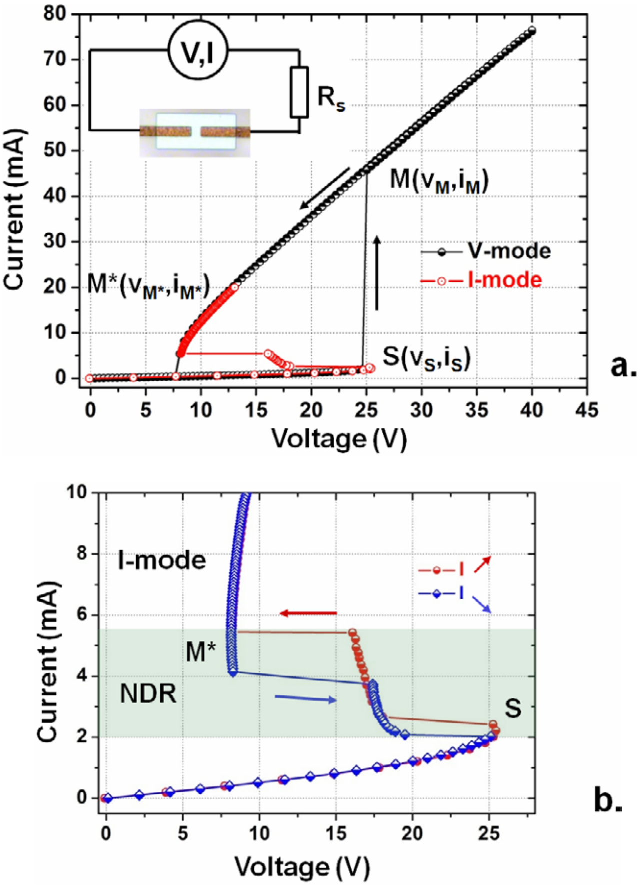

Figure 1. (a) I–V curves (V-mode and I-modes) of a two-terminal VO_2 switch (20-μm length and 20-μm width); the inset shows the VO_2 switch integrated in series with a resistance (R_s) and the voltage or current source. (b) Enlarged view of the I-mode hysteresis indicating the boundaries of the NDR region.

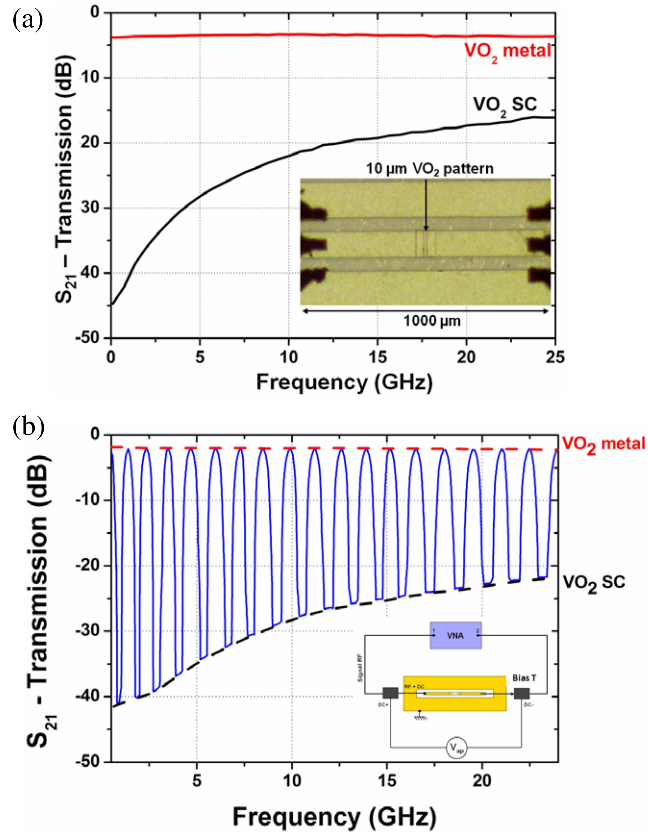

Figure 2. (a) Frequency dependence of the S_{21} transmission parameter for a CPW switch in the off state (VO_2 SC) and in the on state (VO_2 metal). The inset shows an optical microscopy image of the switch. (b) Periodic variation of the S_{21} parameter for a similar CPW switch (with a 20-μm-long VO_2 strip) cycled between the off and on states using a triangular waveform (100 V amplitude, 10 Hz frequency).

line interrupted by a 10-μm-long VO_2 pattern surrounded by two ground lines and overall dimensions adapted to the 50 Ω load (inset in figure 2(a)). In-depth details of the design, fabrication and microwave performance of such devices are given elsewhere [10, 12]. The switching principle and the performance of the obtained device are presented in figure 2(a), which shows the microwave broadband transmission curves, expressed as the transmission parameter S_{21}, versus the frequency. When the VO_2 is in the semiconducting state (SC), the VO_2 line is highly resistive and the switch is in the off state: the microwave signal cannot travel through the device; it is attenuated by more than 15 dB between 100 MHz and 25 GHz (black curve 'VO_2 SC' in figure 2(a)). For a threshold bias voltage of 20 V applied across the VO_2 pattern, VO_2 becomes metallic and the switch is in the on state: the microwave signal is transmitted through the CPW switch with insertion losses of about 3 dB between 100 MHz and 25 GHz (red curve 'VO_2 metal' in figure 2(a)).

Figure 2(b) shows the dynamic behavior of a similar VO_2-based switch with a 20-μm-long VO_2 pattern, expressed as the amplitude variation of the transmitted MW signal (S_{21} parameter) when the MIT transition of the VO_2 pattern is periodically triggered using an ac signal with triangular waveform, 100 V amplitude and 10 Hz frequency. In this case, the S_{21} amplitude varies between the two extreme values that correspond to the semiconducting and metallic states of VO_2 (dashed curves in figure 2(b)).

Devices having the characteristics shown in figure 2 were used for investigating the change in their properties during cycling activation of the VO_2 pattern, in both V- and I-modes. They were integrated in the setup shown in figure 3. It consists of an MW source (Agilent E3633A) operating at 10 GHz—the frequency where the CPW switches have ∼20 dB difference in signal transmission between the on and off states, as observed in figures 2(a) and (b)—connected to the device under test (DUT) via a circulator and a 10 GHz band-pass filter. The VO_2-based device is introduced in a Desert Microwave probe station under dry N_2 atmosphere. The MW signal traveling through the device is detected by a detector (Agilent, B474C) whose output is recorded on an oscilloscope. The MIT in VO_2 is activated by applying a periodic low-frequency voltage or current signal to the two parts of the central signal line of the device, which are interrupted by the VO_2 pattern (inset in figure 2(a)), using a pair of bias Ts. A 500-Ω resistance is included in the external circuit, in series with the VO_2 switch. The activation signal is displayed and recorded on a second channel of the oscilloscope. A computer program automatically acquires the applied low-frequency signal and

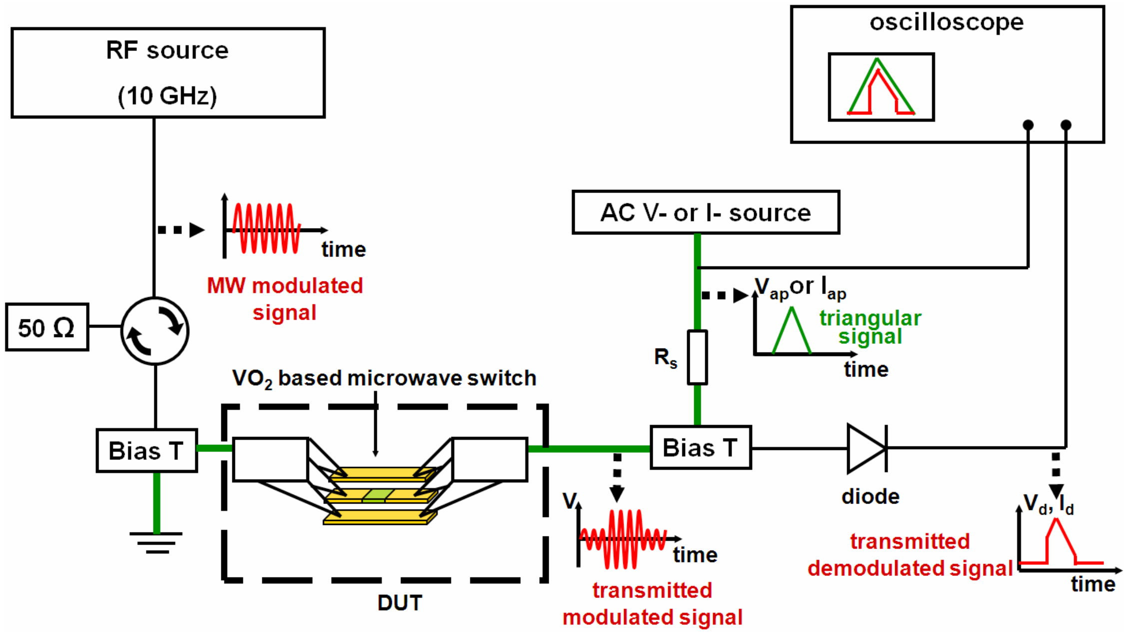

Figure 3. Schematic of the setup used for assessing the lifetime of 10-μm-long VO_2 switches.

the detected MW signal transmitted through the device, allowing the recorded results to be presented in the form shown in figure 4(a) for a voltage-activated device.

3.2.1 Voltage-controlled activation. We first tested the performance of the device shown in the inset of figure 2(a) in the voltage activation mode. For activating the 10-μm-long VO_2 switch, we applied to the device, via the bias Ts, a triangular voltage waveform of 43 Hz frequency and 23.5 V amplitude. As indicated above, when VO_2 is a semiconductor, the MW switch is considered in the off state: the 10 GHz MW signal cannot propagate and no voltage is recorded from the MW detector. For voltages above the threshold value V_s in figure 1 or $V_{ACT\text{-}ON}$ in figure 4(a), VO_2 becomes a metal, the MW signal propagates through the device, the switch is considered in the on state, and a signal is recorded from the MW detector. As shown in figure 4(a), the detected MW signal represented by the red curve allows recording the activation voltage of the device ($V_{ACT\text{-}ON}$) as an indicator of the MIT transition. The second threshold voltage of the control signal, $V_{ACT\text{-}OFF}$, which converts VO_2 back to a semiconductor and corresponds to the M* point in figure 1(a), has not been recorded because its value was too low and comparable with the noise amplitude. Figure 4(b) shows a typical evolution of $V_{ACT\text{-}ON}$ values versus the number of activation cycles. $V_{ACT\text{-}ON}$ remains relatively stable for over 16.25 million activation cycles, with less than 20% variation, mainly because of the MW source instability, and then abruptly drops to zero indicating the device failure. Inspection of the device under an optical microscope revealed a clear degradation of the VO_2 layer, manifested by a change in color and exfoliation, which was likely induced by heat accumulation during the cycling. Indeed, as suggested above, the large hysteresis of the V-mode trace in figure 1(a), and correspondingly, the large hysteresis of the detector response in figure 4(a), suggest a thermally controlled MIT transition.

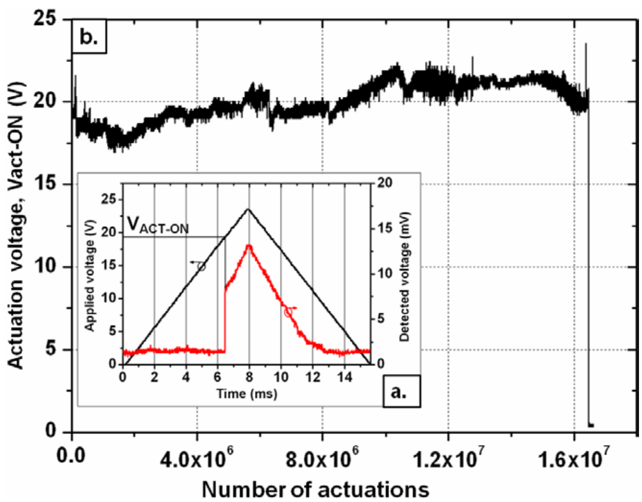

Figure 4. (a) Typical actuation cycle of a voltage-activated 10-μm-long VO_2 switch: the applied voltage signal (black curve) and the MW signal (red curve) detected with the setup of figure 3. (b) Evolution of $V_{ACT\text{-}ON}$ with the number of actuation cycles.

3.2.2 Current-controlled activation. A similar test was performed on an identical device activated in the I-mode. We used a current source (Keithley 6221) delivering a triangular waveform at 1 kHz frequency and 10 mA amplitude to the 10-μm-long VO_2 switch. The applied input current was displayed on the oscilloscope as the potential drop on a 500 Ω series resistance. Prior I–V measurement in the I-mode showed that the threshold current $I_{ACT\text{-}ON}$ (I_S in figure 1) triggering the MIT is ~1 mA. Figures 5(a) and (b) show in a similar manner as figure 4(a) the evolution

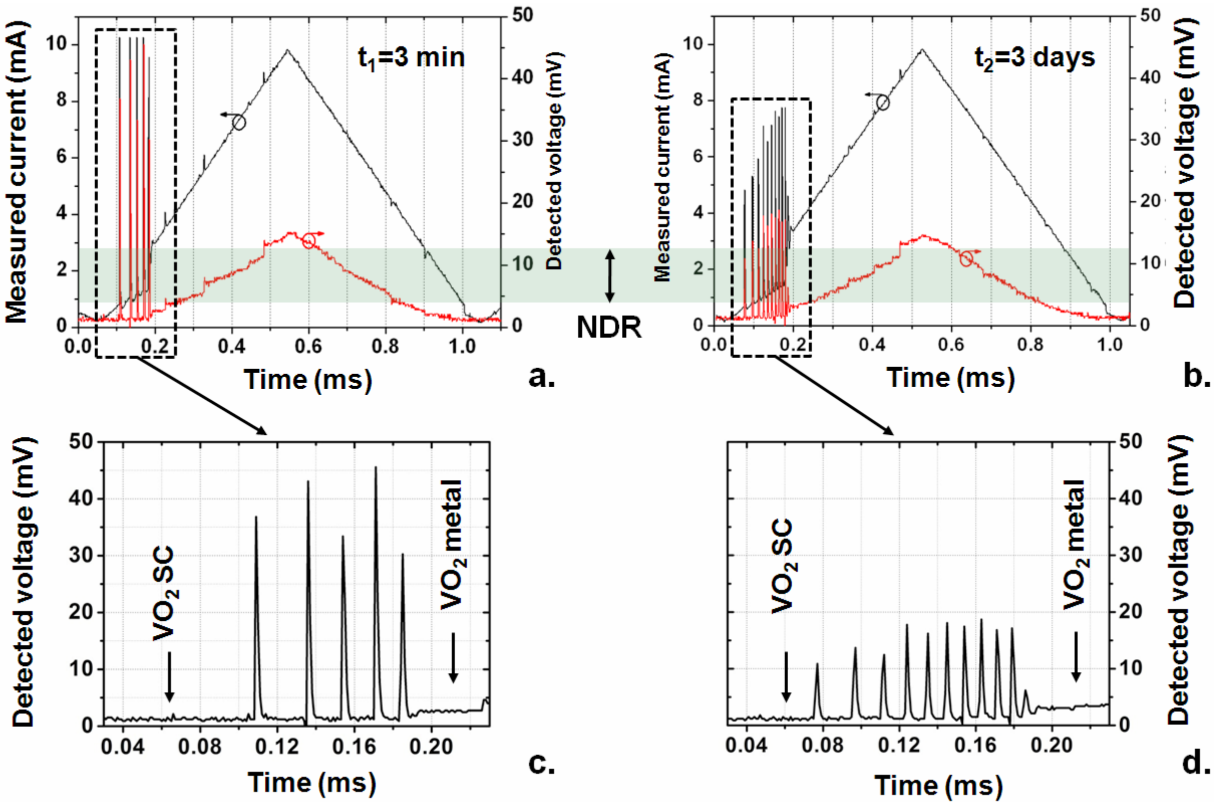

Figure 5. Applied current (black curves, 1 kHz frequency) and MW voltage (red curves) detected from a 10-μm-long VO_2 device, (a) after 3 min of actuation and (b) after more than 250 million actuation cycles. (c) and (d) Magnification of the dashed rectangles in (a) and (b), respectively.

of the detected MW signal (red curves) together with the applied signal ('measured current on R_s', black curves), at the beginning of the test (after 3 min, figure 5(a)) and after more than 250 million current-activation cycles (figure 5(b)). The device sustained more than 260 million cycles with no visible degradation, and further testing was interrupted merely for technical reasons.

The reliability tests described above were conducted on three types of CPW device, having the VO_2 pattern lengths between 10 and 20 μm, in the voltage- and current-controlled regimes. Overall, the lifetime was at least 16 times longer when the VO_2 devices were activated in the current mode than in the voltage mode. As shown in figures 1(a) and (b), the I–V hysteresis is far more pronounced for the V-mode activation; the hysteresis width in this case is defined by the Joule heating when VO_2 is in the metallic state (current values above 45 mA). The hysteresis was narrower for the I-mode activation because of less pronounced resistive heating, as VO_2 becomes metallic at currents above 5 mA. In this case, VO_2 experiences lower thermal stress and lower electric fields, which should reduce the risk of dielectric breakdown, explaining the lifetime enhancement of the current-activated devices.

An interesting feature visible in figures 5(a) and (b) is current-induced self-oscillations in VO_2. These oscillations are marked by dashed rectangles in figures 5(a) and (b) and are magnified in figures 5(c) and (d), respectively; they are related to the NDR region in the I–V curves between 1 and 2.8 mA. Their occurrence depends on several external parameters, such as the amplitude of the activation signal and the value of the series resistance, and was previously observed only for voltage-controlled VO_2 switches [4, 21]. Their onset was explained in terms of the percolative MIT in VO_2, namely, the coexistence of insulator–metallic domains seen as periodic construction–destruction of capacitive phases in the material [4, 20].

The evolution of the detected amplitude and frequency of these self-oscillations during the reliability test is the only sign of fatigue of the tested device. Indeed, as observed in figures 5(c) and (d), the amplitude of self-oscillations decreases from about 42 mV at the beginning of the test to about 17 mV after 250 million current-activation cycles, while their average frequency increases from $\sim$54 to $\sim$84 kHz. These variations can be explained by the resistivity change of VO_2 or by heat accumulation in the device owing to successive current injection. Indeed, this phenomenon was observed in experiments were we induced self-oscillations in a two-terminal VO_2 switch of 5-μm length and 20-μm width by applying a square-shaped current signal (100 Hz, 2 mA amplitude) within the NDR region of the device. The applied current signals as well as the oscillations induced in the VO_2 switch, represented as voltage detected across the series resistance, are plotted in figure 6(a).

The amplitude and frequency of these oscillations depend, among other parameters, on the temperature of the VO_2 switch, as shown in figure 6(b) for the 5-μm-long

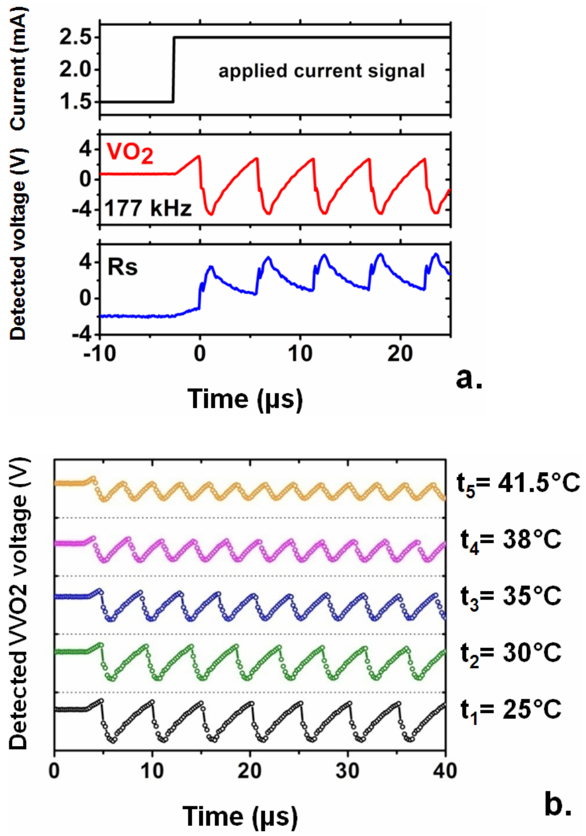

Figure 6. (a) Typical self-oscillations induced by a square-shaped current waveform (100 Hz, 2 mA amplitude) in a 5-μm-long, 20-μm-wide two-terminal VO_2 switch; panel (b) shows the oscillations with temperature from $t_1 = 25\,^{\circ}C$ to $t_5 = 41.5\,^{\circ}C$.

VO_2 switch for temperatures ranging from $t_1 = 25\,^{\circ}C$ to $t_5 = 41.5\,^{\circ}C$. The amplitude of the oscillations decreases by 60% (from 6.6 to 2.6 V) with increasing temperature from t_1 to t_5, whereas their frequency increases by 40% (from $\sim$0.2 to $\sim$0.3 MHz). The variation of the parameters of the self-oscillations appearing during the current-activation of VO_2 switches is thus a very fine indicator of the changes induced in the VO_2 material. This property can be further exploited for the use of these devices as temperature, pressure or gas sensors.

4. Conclusions

We investigated the reliability and lifetime of the MIT in two-terminal VO_2 switches under multiple cycles of voltage- and current-induced activation. The lifetime was at least 16 times longer for the current-driven than the voltage-driven VO_2 devices; current-induced activation is less affected by thermal effects, resulting in a smaller degradation of the VO_2 films. This activation scheme is accompanied by electrical self-oscillations induced in the VO_2-based switch, which are a fine indicator of the modification of material properties. The presented results demonstrate the potential for the integration of VO_2 thin films in devices for advanced applications requiring a large number of stable and reproducible switching cycles.

Acknowledgment

This work was supported by ANR-France through the project 'Admos-VO_2', ANR 07-JCJC-0047JC.

References

[1] Morin F 1959 *Phys. Rev. Lett.* **3** 34
[2] Stefanovich G, Pergament A and Stefanovich D 2000 *J. Phys.: Condens. Matter* **12** 8837
[3] Kim H T, Chae B G, Youn D H, Maeng S L, Kim G, Kang K Y and Lim Y S 2004 *New J. Phys.* **6** 52
[4] Kim H-T, Kim B-J, Choi S, Chae B-G, Lee Y W, Driscoll T, Qazilbash M M and Basov D N 2010 *J. Appl. Phys.* **107** 023702
[5] Cavalleri A, Tóth C S, Siders C W, Squier J A, Ráksi F, Forget P and Kieffer J C 2001 *Phys. Rev. Lett.* **87** 237401
[6] Rini M, Cavalleri A, Schoenlein R W, López R, Feldman L C, Haglund R F Jr, Boatner L A and Haynes T E 2005 *Optics Lett.* **30** 558
[7] Kikuzuki T and Lippmaa M 2010 *Appl. Phys. Lett.* **96** 132107
[8] Sahana M B, Subbanna G N and Shivashankar S A 2002 *J. Appl. Phys.* **92** 6495
[9] Kim C, Shin J S and Ozaki H 2007 *J. Phys.: Condens. Matter* **19** 096007
[10] Dumas-Bouchiat F, Champeaux C, Catherinot A, Crunteanu A and Blondy P 2007 *Appl. Phys. Lett.* **91** 223505
[11] Pergament A L, Boriskov P P, Velichko A A and Kuldin N A 2010 *J. Phys. Chem. Solids* **71** 874
[12] Dumas-Bouchiat F, Champeaux C, Catherinot A, Givernaud J, Crunteanu A and Blondy P 2009 *Materials and Devices for Smart Systems III* ed J Su, L-P Wang, Y Furuya, S Trolier-McKinstry and J Leng (*Mater. Res. Soc. Symp. Proc.*) **1129** 275
[13] Givernaud J, Crunteanu A, Orlianges J-C, Pothier A, Champeaux C, Catherinot A and Blondy P 2010 *IEEE Trans. Microwave Theory Tech.* doi 10.1109/TMTT.2010.2057172
[14] Driscoll T, Kim H-T, Chae B-G, Kim B-J, Lee Y-W, Marie Jokerst, Palit S, Smith D R, Di Ventra M and Basov D N 2009 *Science* **325** 1518
[15] Wen Q-Y, Zhang H-W, Yang Q-H, Xie Y-S, Chen K and Liu Y-L 2010 *Appl. Phys. Lett.* **97** 021111
[16] Kim D 2009 *34th Int. Conf. Infrared, Millimeter, and Terahertz Waves, IRMMW-THz* art. no. 5324735
[17] Guzman G, Beteille F, Morineau R and Livage J 1996 *J. Mater. Chem.* **6** 505
[18] Ilinski A, Silva-Andrade F, Shadrin E and Klimov V 2004 *J. Non-Cryst. Solids* **338–340** 266
[19] Ko C and Ramanathan S 2008 *J. Appl. Phys.* **104** 086105
[20] Rozen J, Lopez R, Haglund R F and Feldman L C 2006 *Appl. Phys. Lett.* **88** 081902
[21] Sakai J 2008 *J. Appl. Phys.* **103** 103708